

Anisotropy of Passive and Active Rat Vagina under Biaxial Loading

Alyssa Joan Huntington

Thesis submitted to the faculty of the Virginia Polytechnic Institute and State University in
partial fulfillment of the requirements for the degree of

Master of Science
In
Engineering Mechanics

Raffaella De Vita
Vincent M. Wang
Jonathan B. Boreyko

April 13, 2018
Blacksburg, Virginia

Keywords: vagina, biaxial mechanical characterization, contractile force

Anisotropy of Passive and Active Rat Vagina under Biaxial Loading

Alyssa Huntington

ABSTRACT

Pelvic organ prolapse, the descent of the pelvic organs from their normal anatomical position, is a common condition among women that is associated with mechanical alterations of the vaginal wall. In order to characterize the complex mechanical behavior of the vagina, we performed planar biaxial tests of vaginal specimens in both the passive (relaxed) and active (contracted) states. Specimens were isolated from virgin, female Long-Evans rats ($n=16$) and simultaneously stretched along the longitudinal direction (LD) and circumferential direction (CD) of the vagina. Tissue contraction was induced by electric field stimulation (EFS) at incrementally increasing values of stretch and, subsequently, by KCl. On average, the vagina was stiffer in the CD than in the LD ($p<0.001$). The mean maximum EFS-induced active stress was significantly higher in the CD than in the LD ($p<0.001$). On the contrary, the mean KCl-induced active stress was lower in the CD than in the LD ($p<0.01$). When comparing the mean maximum EFS-induced active stress to the mean KCl-induced active stress, no differences were found in the CD ($p=0.404$) but, in the LD, the mean active stress was much higher in response to the KCl stimulation ($p<0.001$). Collectively, these results demonstrate that the anisotropic behavior of the vaginal tissue is determined not only by the collagen and smooth muscle fiber organization but also by the innervation. The findings of this study may contribute to the development of more effective treatments for pelvic organ prolapse.

Anisotropy of Passive and Active Rat Vagina under Biaxial Loading

Alyssa Huntington

GENERAL AUDIENCE ABSTRACT

Pelvic organ prolapse (POP), the descent of the pelvic organs from their normal anatomical position, is a common condition among women that is associated with alterations of the mechanical properties of the vaginal wall. The characterization of the mechanical properties of the vagina is crucial for the development of effective treatments for POP. Biaxial tensile tests were performed in this study so we could observe the behavior of the vagina along both the circumferential direction (CD) and the longitudinal direction (LD). In these tests, square specimens were secured along all four edges and pulled outward such that we could observe the relationship between the stretch and the stress that the tissue experienced. Additionally, because the vagina contains smooth muscle, we also tested the tissue in its active, or contractile state at each stretch level. Contractions were induced by applying electric field stimulation (EFS) to observe nerve-mediated responses, and subsequently by potassium chloride (KCl). On average, the vagina was stiffer in the CD than in the LD ($p < 0.001$). The mean maximum EFS-induced active stress was significantly higher in the CD than in the LD ($p < 0.001$). On the contrary, the mean KCl-induced active stress was lower in the CD than in the LD ($p < 0.01$).

ACKNOWLEDGEMENTS

I would like to acknowledge the contribution of Dr. Emanuele Rizzuto from La Sapienza University to the work here presented.

Additionally, I would like to thank the National Science Foundation for funding this project under grant number 1511603.

TABLE OF CONTENTS

Introduction.....	1
Materials and Methods.....	3
Results	8
Discussion	15
References	19

LIST OF FIGURES

Figure 1: Schematic of specimen preparation. (a) The rat vagina is cut along the urethra in the LD to isolate a square specimen with sides that are parallel to LD and CD of the vagina. (b) The vaginal tissue specimen is hooked to custom-made clamps.	3
Figure 2: (a) Custom-built biaxial tensile machine consisting of four linear actuators, two load cells, four 3-D printed clamps, and a bath. (b) Schematic of the electrodes used for EFS.	5
Figure 3: (a) Schematic of the incremental stretching protocol used to obtain passive and EFS-induced active force data simultaneously along the LD and CD. Red square symbols denote the application of EFS. (b) Schematic of the load and applied EFS at each stretch. (c) Schematic of the load and applied KCl stimulation following the incremental stretching protocol and EFS.	7
Figure 4: Mean (\pm S.E.M.) passive stress versus stretch data along the LD and CD of the vaginal specimens (n=16). ***, $p < 0.001$	9
Figure 5: EFS induced forces of a representative specimen at stretch values of (a) 1, (b) 1.2, and (c) 1.42. The time scales are adjusted so that $t=0$ represents 1 s prior to the application of the EFS. Thus, the forces at $t=0$ are the passive forces.	10
Figure 6: Mean (\pm S.E.M.) EFS induced active stresses versus stretches in the LD and CD (n=16). ****, $p < 0.0001$	11
Figure 7: Mean (\pm SEM) stretch at which maximum EFS induced active force was recorded (n=16). **, $p < 0.01$	12`
Figure 8 Force for a representative specimen during the application of the KCl stimulation. In this figure, the time scale is adjusted so that $t=0$ represents the time in which the solution used for EFS stimulation was removed before adding the KCl-based solution.	13
Figure 9 Mean (\pm SEM) maximum active stresses in response to EFS and active stresses in response to KCl stimulation in the LD and CD (n=16). **, $p < 0.01$	14
Figure 10 Figure 10: Mean (\pm SEM) maximum active stress obtained by EFS normalized by active stress obtained by KCl-induced stimulation in the LD and CD (n=16). ***, $p < 0.001$	14

LIST OF TABLES

Table 1: Mean \pm S.D. rat vagina specimen dimensions (n=16). The thickness was measured to be 0.38 ± 0.13 mm.	8
---	---

Introduction

Pelvic organ prolapse (POP) represents a major public health concern in adult women worldwide. Prolapse occurs when a pelvic organ, such as the bladder or uterus, descends from its normal position. This can cause urinary incontinence, fecal incontinence, pelvic discomfort, sexual dyspareunia, and a decreased quality of life ^{12, 26}. Treatments for POP include non-surgical management techniques such as pelvic floor muscle training, the use of pessaries, lifestyle changes as well as surgical options ¹. Surgeries have limited success, though, with nearly 30% of POP surgical patients returning for additional operations to treat recurrent prolapse ³⁶. While it is understood that factors such as age, weight, and parity are strongly associated with the development of POP, the exact underlying causes of POP remain unknown ^{11, 48}. However, several studies have indicated that the structural and mechanical properties of the vagina are altered in women with POP.

The vagina is comprised of four layers: the epithelium, the subepithelium, the muscularis, and the adventitia ³³. Structurally, the most important layers are the subepithelium, which is made up of collagen, and the muscularis, which contains longitudinally and circumferentially oriented smooth muscle cells ⁵³. The collagen content determines the passive mechanical properties of the vagina, and the smooth muscle content dictates the active, or contractile, mechanical properties. There is a wide range of findings in regard to structural changes of the vagina associated with POP. Vaginal specimens with POP have been reported to have both increased ³³ and decreased ³¹ levels of collagen III, the predominant collagen throughout the vaginal wall. Several studies have reported significantly decreased fractions of smooth muscle in vaginal tissue with POP ^{3, 7, 23, 49}. In addition, collagen and smooth muscle have been reported being less organized in prolapsed tissues ^{8, 23}. Of

course, changes in collagen and smooth muscle content and orientation lead to altered passive and active mechanical properties of the vagina.

The influence of several factors on the passive mechanics of the vagina has been studied including prolapse^{20, 25, 38, 44}, pregnancy and parity^{17, 28, 40, 46, 52}, age⁹, menopause and hormones^{15, 18, 22, 29, 30}, and weight³². Additionally, a few studies have been conducted to observe how the passive mechanical behavior of the vagina differs regionally across the entire vagina^{45, 51}. With the exception of a few studies^{24, 50, 37}, the overwhelming majority of these studies were conducted using uniaxial tensile tests, in which vaginal strips from along either the LD or the CD were tested. In addition to the passive behavior of vagina, the presence of smooth muscle in the tissue calls for the characterization of the active, or contractile, properties. Active studies have been performed using exclusively uniaxial tests. Contractions have been induced using high concentrations of KCl to observe contractions caused by direct membrane depolarization^{4, 6, 16, 19, 53}, electric field stimulation (EFS) for nerve-mediated responses⁵⁴, various agonists and antagonists for receptor-mediated responses, or combinations thereof^{5, 21, 27, 34, 35, 47}. Finally, there have been several *in vivo* tests that measure the mechanical properties of the vagina using inflation or suction techniques^{2, 10, 13, 14, 42}. Although these tests better emulate *in vivo* loading conditions, they do not allow for distinction and quantification of the active and passive properties of the vaginal tissue. In this study, we provide the first planar biaxial characterization of both passive and active properties of the vagina using the rat as an animal model. Additionally, we utilized EFS followed by KCl to induce contractions of the vaginal tissue in order to compare nerve-mediated mechanical responses to those caused by direct membrane depolarization. The findings of this rigorous mechanical characterization, which includes the study of the anisotropic behavior of the vagina in both the passive and active states, will serve to develop new effective treatments for POP.

Materials and Methods

This study was conducted with the approval of the Institutional Animal Care and Use Committee (IACUC) at Virginia Tech. A total of sixteen adult female Long-Evans rats, aged between 70-89 days, were used for this study. After euthanizing each rat via decapitation, the entire vagina was immediately isolated. During the dissection, the vagina was continuously kept moist with Krebs-Ringer Bicarbonate Buffer. The vaginal canal was opened into a flat specimen by placing a cut along the urethra. It was then trimmed to be approximately square with sides parallel to the longitudinal direction (LD) and the circumferential direction (CD) of the vagina (Figure 1). Two small hooks (size 18 dry fly hook, Mustad) that were connected via a silk thread were placed on each side of the specimen.

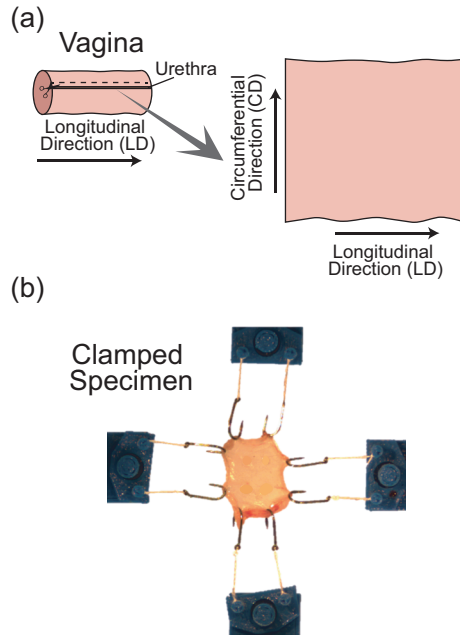


Figure 1: Schematic of specimen preparation. (a) The rat vagina is cut along the urethra in the LD to isolate a square specimen with sides that are parallel to LD and CD of the vagina. (b) The vaginal tissue specimen is hooked to custom-made clamps.

The specimen was then secured to a custom-built biaxial testing machine described in detail elsewhere (Figure 2(a))⁵⁵. The linear actuators (T-NA08A25, Zaber Technologies, Inc.) of the

biaxial system had a maximum travel length of 25 mm and micro-step size resolution of 0.048 μm while the two load cells (FSH02663, Futek Advanced Sensor Technology, Inc) had a maximum load capacity of 50 g and accuracy of $\pm 0.1\%$.

Once mounted on the biaxial testing machine, each specimen was submerged in a bath of Krebs-Ringer bicarbonate buffer with calcium (2.00 mM). In order to establish the initial configuration more consistently across different specimens, each specimen was stretched with a displacement rate of 0.05 mm/s until a pre-load of approximately 4 mN was recorded in both axial loading directions. It was then allowed to relax for 30 minutes before being re-stretched at 0.05 mm/s displacement rate until a 4 mN preload was reached in both directions. In this configuration, a picture of each specimen was quickly taken using a CMOS camera (DCC1545M, Thorlabs) equipped with lens (59-871, Edmund Optics) to measure the specimen dimensions using ImageJ (NIH, Bethesda, MD). Specifically, the average of two distances between the hooks that were placed directly opposite of each other along the LD or CD was considered to be the initial side-length of the specimen in that direction (Table 1). In this initial configuration, the specimen was then electrically stimulated in the LD and CD using a high-power pulse stimulator (701C, Aurora Scientific, Inc.) through custom made stainless steel electrodes (Figure 2(b)). The electrodes were designed such that one plate could be positioned directly above the specimen and the other plate directly below the specimen. This design ensured that the direction of the electric current would be perpendicular to both the LD and CD and applied through the specimen thickness. The EFS consisted of one train of 2 ms pulses delivered at 70 Hz for 0.8 s, with 700 mA of current intensity. These EFS parameters were selected since they produced maximum forces in preliminary tests.

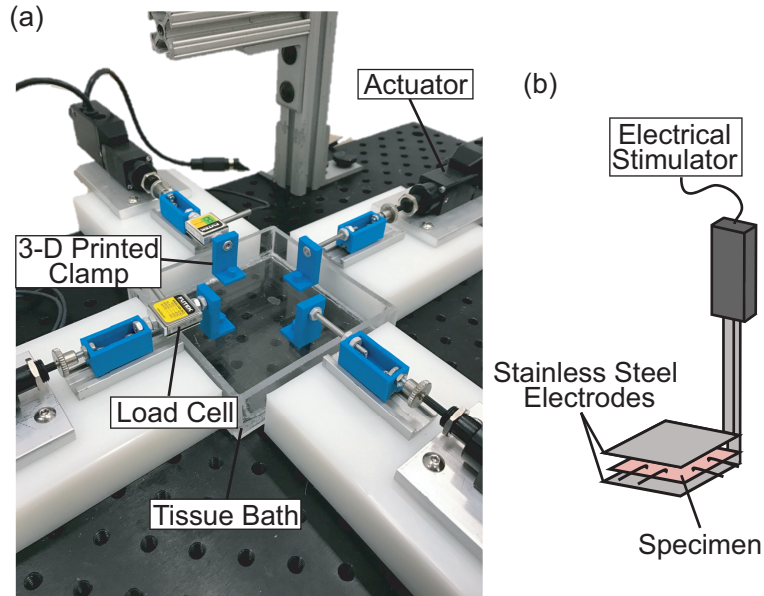


Figure 2: (a) Custom-built biaxial tensile machine consisting of four linear actuators, two load cells, four 3-D printed clamps, and a bath. (b) Schematic of the electrodes used for EFS.

Each specimen was then stretched simultaneously in each direction by increasing the length of the specimen by 2% of its initial LD and CD lengths for 21 consecutive increments to a final stretch of 42%. The specimen was held at each stretch for 90 seconds and, at the end of each holding period, the forces in the LD and CD were measured. These forces were the “passive forces” of the specimen, i.e. the forces that resulted from the application of the stretches prior to the EFS. Note that these are not fully passive because the smooth muscle was not chemically passivated. After each holding period, the specimen was electrically stimulated using the same methods and parameters presented above and the contraction forces in the LD and CD were measured. At each stretch, the “active force” in the LD or CD was defined as the difference between the maximum force reached via EFS and the passive force at that stretch. A schematic of this testing protocol is presented in Figure 3(a)-(b).

After electrically stimulating the specimen multiple times, the specimen was unloaded until the load reached about 4 mN and it was then allowed to relax for 5 minutes. While recording force data, the testing solution was removed and replaced with Krebs-Ringer bicarbonate buffer with

calcium (2.00 mM) and a high concentration of potassium chloride (124 mM) (Figure 3(c))²¹. The specimen remained in the bath until the force in the LD and CD reached a maximum value and began to decrease, which typically took 1-2 minutes. The “active force” due to the KCl in the LD or CD was calculated as the difference between the maximum force reached with the KCl stimulation and the passive force recorded before the KCl solution was added (Figure 3(c)). Specimen thickness was measured immediately after testing in 5 different locations through the use of a CCD laser displacement sensor (LK-G82, Keyence, Inc.) with an accuracy of 7.5 μm (Table 1). It was assumed that changes in thickness during biaxial testing were negligible. Cross sectional area was measured as the average of distances between hooks on the same side multiplied by specimen thickness. Passive and active force data in the LD or CD were divided by the cross-sectional area that was perpendicular to the LD or CD, respectively, to obtain passive (nominal) and active stress data.

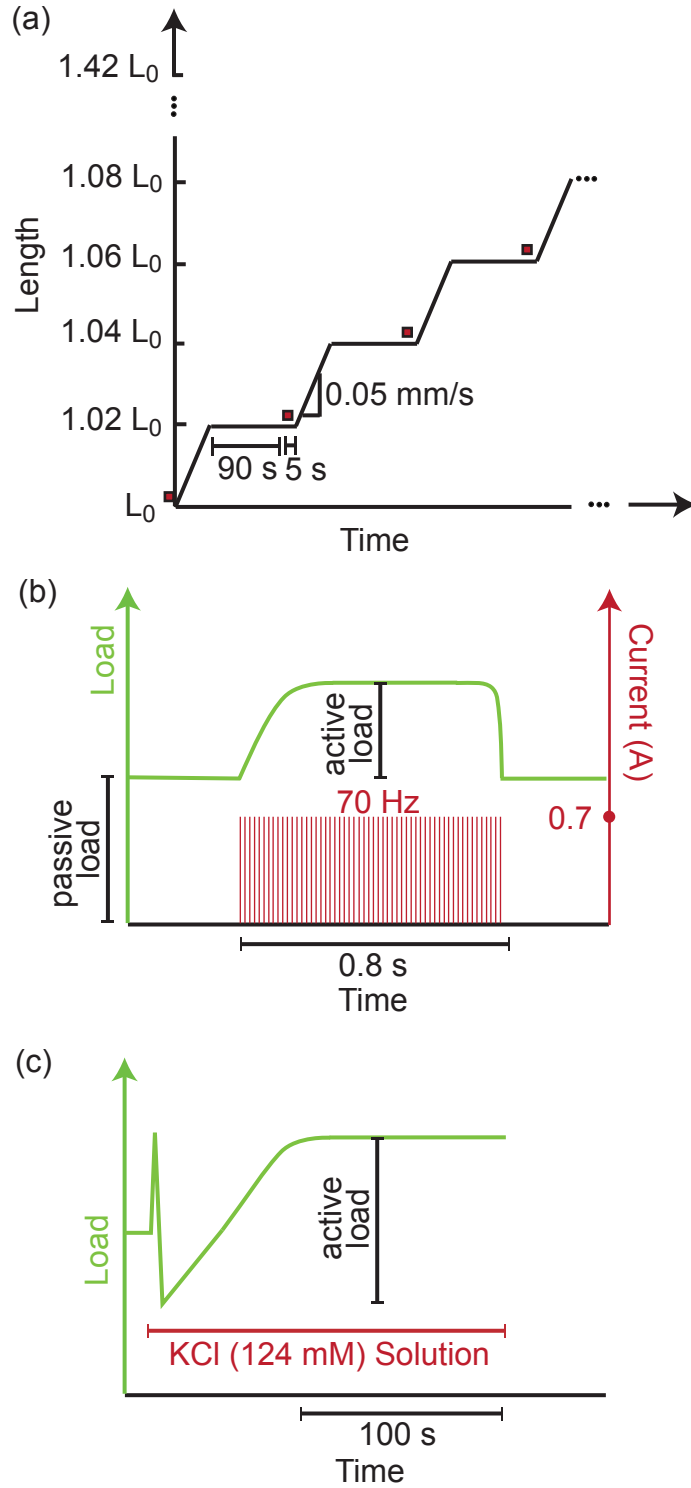


Figure 3: (a) Schematic of the incremental stretching protocol used to obtain passive and EFS-induced active force data simultaneously along the LD and CD. Red square symbols denote the application of EFS. (b) Schematic of the load and applied EFS at each stretch. (c) Schematic of the load and applied KCl stimulation following the incremental stretching protocol and EFS.

Statistical Analysis

Maximum active stresses induced by EFS or KCl, stretches at which the maximum EFS-induced active stresses were achieved, and maximum EFS-induced active stresses normalized by KCl induced active stresses were compared between the LD and CD using Wilcoxon signed-rank tests. Similarly, in each direction, the maximum EFS-induced and KCl-induced active stresses were compared. Differences in passive stresses and EFS-induced active stresses were evaluated with 2-way ANOVA using direction and stretch as factors. Statistical analysis was performed with GraphPad Prism 6.0, and differences were considered significant when $p < 0.05$.

	Initial side-length (mm)	Hook distance (mm)	Cross-sectional Area (mm ²)
LD	10.54±1.18	7.04±0.72	2.67±0.88
CD	11.10±1.11	6.62±0.87	2.55±1.05

Table 1: Mean \pm S.D. rat vagina specimen dimensions ($n=16$). The thickness was measured to be 0.38 ± 0.13 mm.

Results

The mean passive stress-stretch data collected from $n=16$ specimens in both loading directions are shown in

Figure 4. The rat vaginal tissue exhibits the typical non-linear stress-stretch behavior of soft biological tissues. The 2-way ANOVA revealed that *direction* ($p < 0.001$) and *stretch* ($p < 0.0001$) significantly affected the passive force. As expected, the mean passive force increased as the stretch increases. More interestingly, the tissue resulted to be anisotropic, being, on average, stiffer in the CD than in the LD.

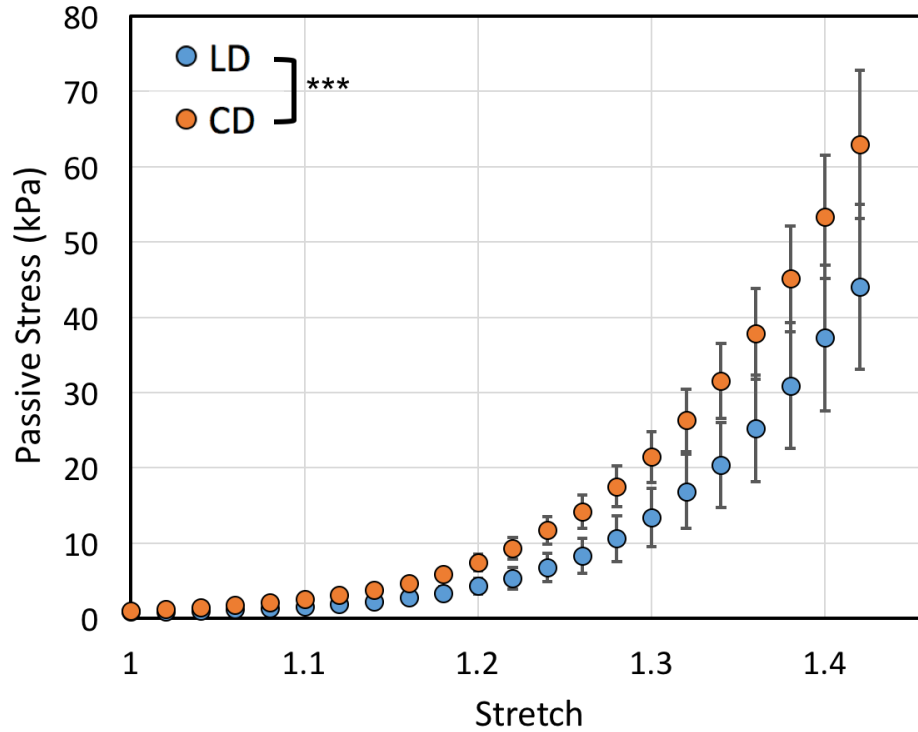


Figure 4: Mean (\pm S.E.M.) passive stress versus stretch data along the LD and CD of the vaginal specimens ($n=16$). ***, $p<0.001$.

Force vs. time data collected during the first, middle, and last EFSs corresponding to stretch values of $L = L_0$, $=1.2 L_0$, and $=1.42 L_0$ are shown for a representative specimen in Figure 5. After the EFS was applied ($t=1$ s in Figure 5(a), (b), and (c)) the vagina contracted producing gradual increases in forces in the LD and CD until the stimulation ended ($t=1.8$ s in Figure 5(a), (b), and (c)) and, at that time, the forces returned to their passive values. At $L=1 L_0$, the specimen was pre-loaded so that the initial passive forces acting along each direction were nearly identical, around 4 mN (Figure 5(a)). As the stretch increased, the difference between the passive forces along the CD and LD increased with higher passive forces in the CD than in the LD (Figure 5(b)-(c)). The active

forces were typically higher in the CD than in the LD at each stretch value. The differences of both active and passive forces in the two directions demonstrate the anisotropy of the vaginal tissue.

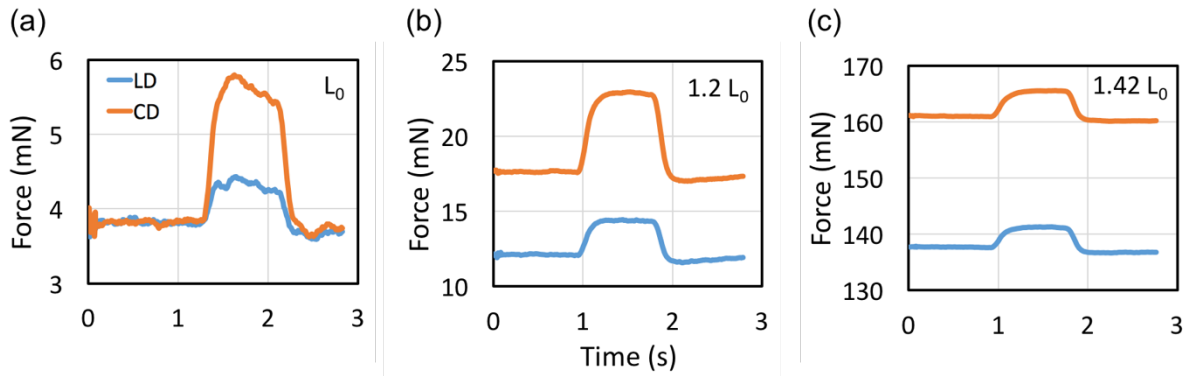


Figure 5: EFS induced forces of a representative specimen at stretch values of (a) 1, (b) 1.2, and (c) 1.42. The time scales are adjusted so that $t=0$ represents 1 s prior to the application of the EFS. Thus, the forces at $t=0$ are the passive forces.

The mean active stresses in response to EFS at each stretch value tested are shown in

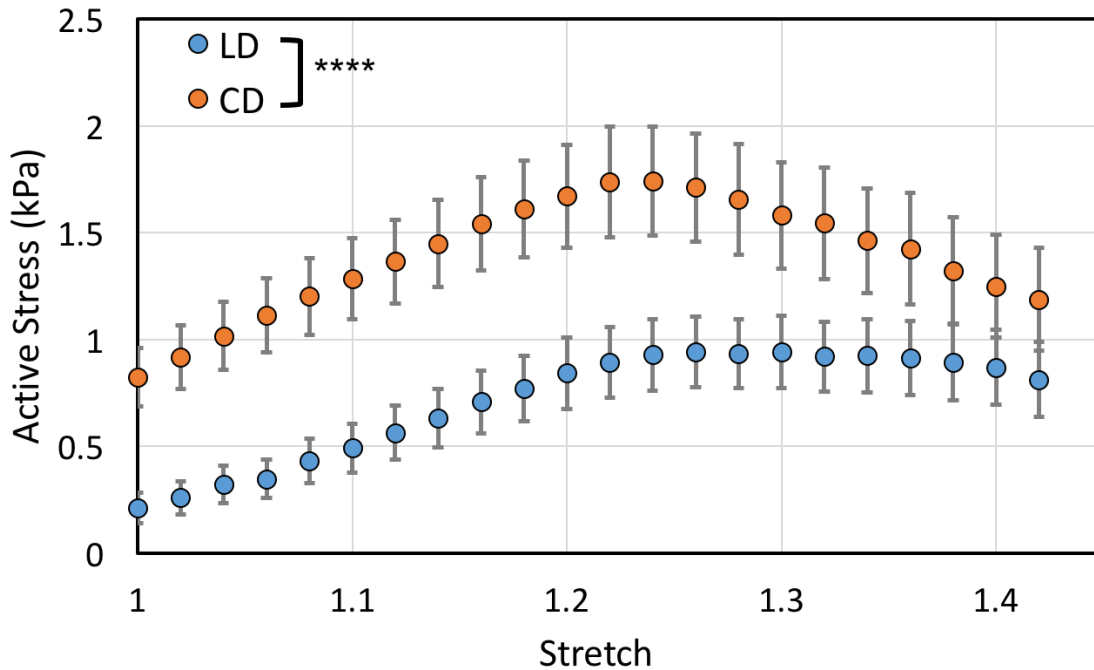


Figure 6. The 2-way ANOVA revealed that the stretch ($p<0.0001$) and direction ($p<0.0001$) factors significantly affected the active stress. EFS-induced active stresses were higher in the CD than in

the LD, increasing with stretch until the maximum values were reached. These stresses then decreased even though the stretch continued to increase. The maximum active stress induced by EFS was about 60% higher in the CD than in the LD ($p<0.001$) The maximum active stress along the LD was measured at a stretch of about 1.32 on average, while the maximum active stress along the CD was obtained at a stretch of around 1.25 on average (Figure 7). This difference was found to be statistically significant ($p<0.01$).

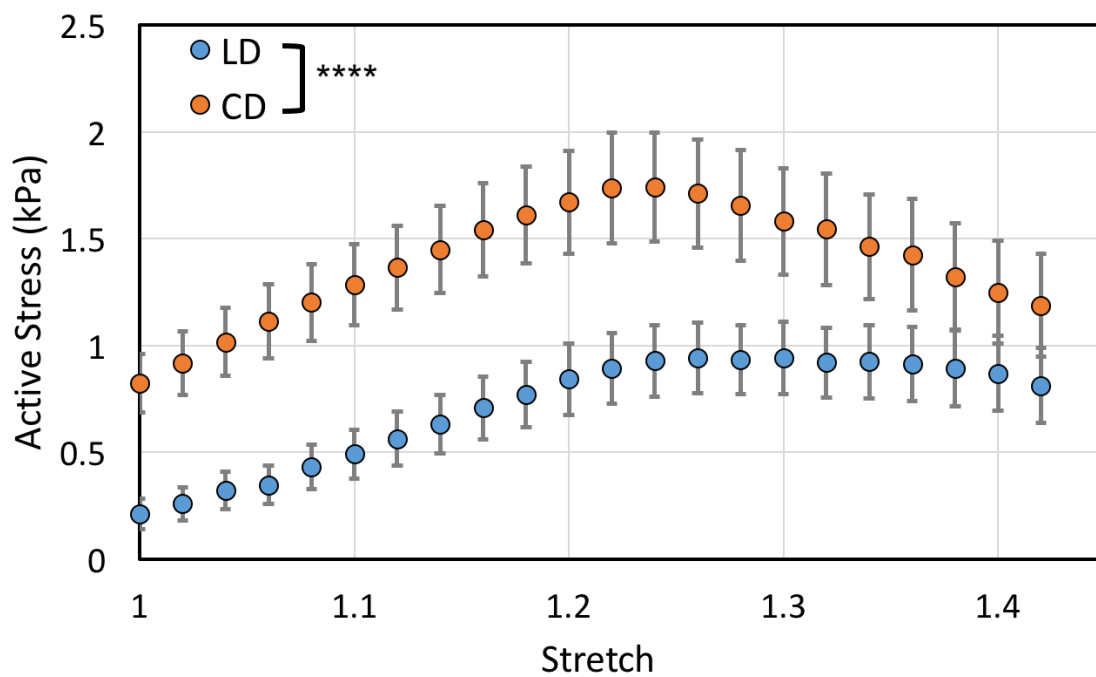
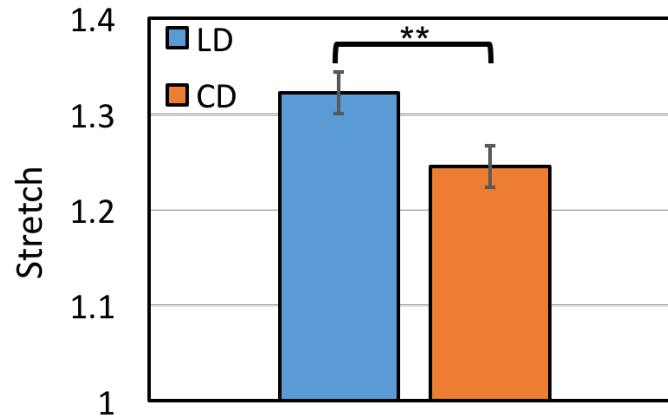


Figure 6: Mean (\pm S.E.M.) EFS induced active stresses versus stretches in the LD and CD ($n=16$). ****, $p<0.0001$.



*Figure 7: Mean (\pm SEM) stretch at which maximum EFS induced active force was recorded ($n=16$).
**, $p<0.01$.*

In Figure 8, the forces along the LD and the CD for a representative specimen that was stimulated using KCl are reported. During the first few seconds of KCl stimulation, the forces in both the LD and CD quickly increased and decreased due to the removal of the first solution and the addition of the KCl solution. Once the KCl solution was added, the forces in each direction gradually increased until plateauing after around 100 s.

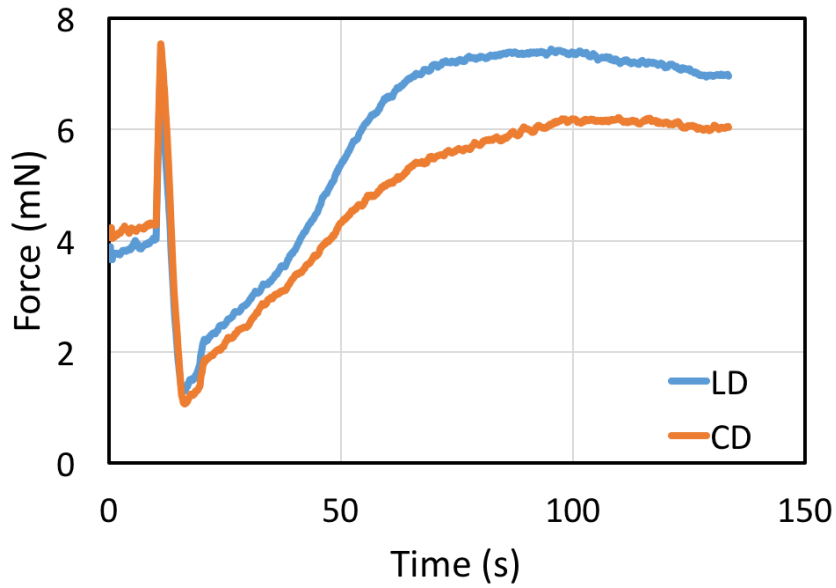


Figure 8 Force for a representative specimen during the application of the KCl stimulation. In this figure, the time scale is adjusted so that $t=0$ represents the time in which the solution used for EFS stimulation was removed before adding the KCl-based solution

On average, the KCl stimulation caused 60% higher active stresses in the LD than in the CD ($p<0.01$). The mean active stresses caused by the KCl stimulation were 3.46 kPa in the LD, and 2.15 kPa in the CD (**Error! Reference source not found.9**). When comparing the mean maximum active force induced by EFS to the mean active force induced by the KCl, no differences were found in the CD ($p=0.404$). On the other hand, in the LD, the mean active force was much higher in response to the KCl stimulation than to in response to EFS ($p<0.001$). All statistically significant differences found with respect to stimulation methods and direction are noted in Figure 9. Finally, the mean maximum EFS- induced active stress normalized by the KCl-induced active stress was significantly higher in the CD than the LD (Figure 10).

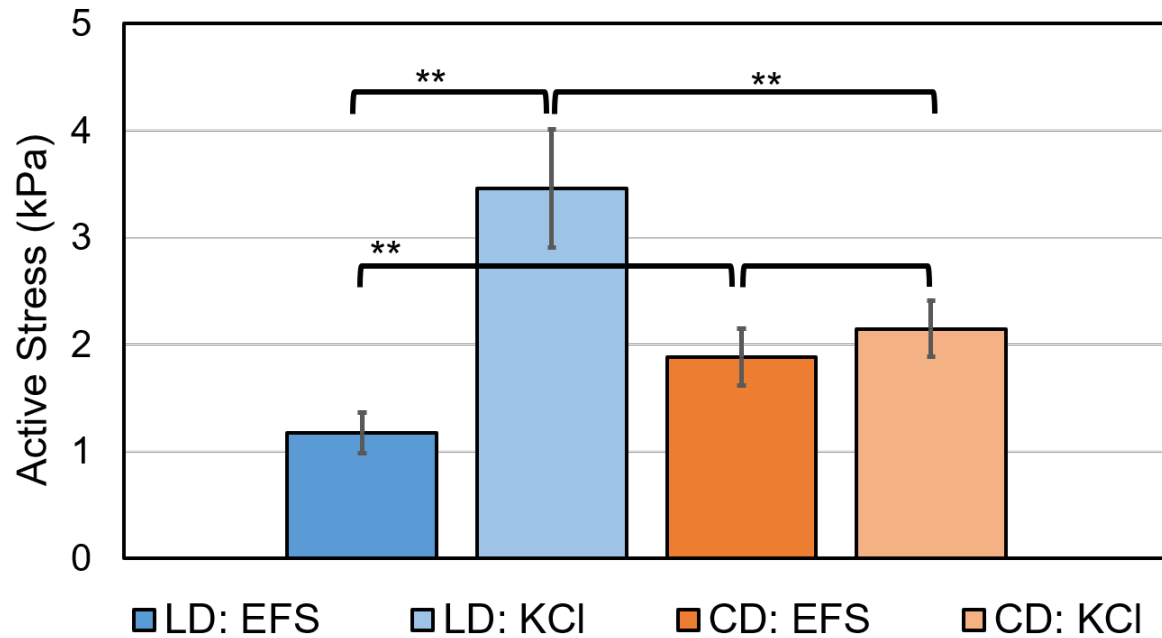


Figure 9 Mean (\pm SEM) maximum active stresses in response to EFS and active stresses in response to KCl stimulation in the LD and CD ($n=16$). **, $p<0.01$.

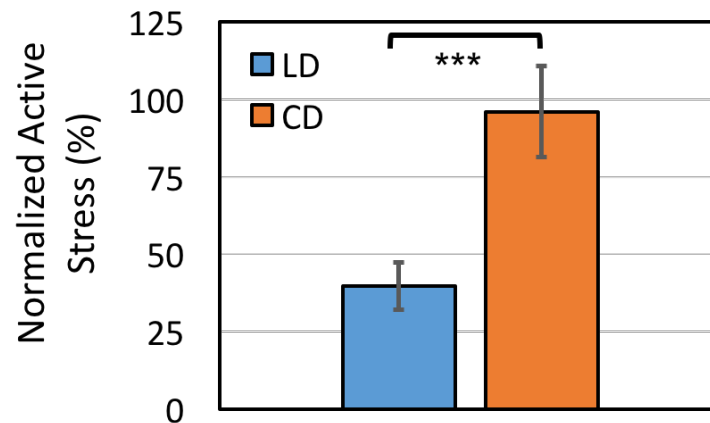


Figure 10 Figure 10: Mean (\pm SEM) maximum active stress obtained by EFS normalized by active stress obtained by KCl-induced stimulation in the LD and CD ($n=16$). ***, $p<0.001$.

Discussion

In this study, we presented the first characterization of the biaxial passive and active mechanical properties of the rat vagina. The mechanical properties of this reproductive organ are crucial to the proper function of the entire female pelvic floor. Indeed, alterations of these properties are implicated in the development of pelvic floor disorders such as sexual dysfunction, urinary incontinence, and prolapse. The vagina is a tubular organ that, in vivo, is primarily loaded along the LD and CD, and smooth muscle fibers within the muscularis layer of the vagina are mainly oriented along these directions. The vagina is widely assumed to be anisotropic, but very few tests have sought to quantify this behavior. For these reasons, we performed planar biaxial tests, rather than the commonly used uniaxial tests, to quantify the mechanical behavior of the vagina. During mechanical testing, we stimulated the vaginal tissue through nerve fibers using EFS and through direct membrane depolarization using KCl. Our findings demonstrated that vaginal tissue is highly anisotropic: the tissue in the CD is significantly stiffer than in the LD in the passive state (Figure 4) and EFS-induced active state (Figures 6). However, the vaginal tissue generated higher stress in the LD when activated via KCl (Figure 9).

Previous studies have sought to quantify the anisotropy of vaginal tissue in the passive state by comparing results of uniaxial tests collected from tissue strips that were cut along the LD and CD^{39, 43, 45}, and, very recently, through inflation-extension testing⁴¹. The results from these studies have been conflicting, though. Pena *et al.* found that the vagina was stiffer in the LD than in the CD³⁹. Rubod *et al.* reported that the anisotropy of the vaginal tissue was strain-dependent: there were no significant differences in stiffness at strains below 50%, but the tissue in the LD became stiffer at higher strains^{43, 45}. Similarly, Robison *et al.* also found the vagina to be stiffer in the LD at high strains, but found it stiffer in the CD at low strains⁴¹. In this study, we found that, on

average, the rat vagina was significantly stiffer in the CD at strains between 0 and 42% (Figure 4). However, it should be noted that not every specimen followed this trend, as there were some specimens that exhibited higher stresses in the LD than in the CD for the same stretches. Our anisotropy findings align with those of Robison *et al.* [6] but additional testing at higher strains would need to be performed to potentially observe the reported strain-dependent anisotropy of vaginal tissue. The stress values reached during our testing were lower than previously reported stresses at similar strains⁴⁰. This is likely due to our incremental protocol that allowed the specimens to relax significantly throughout the test.

The mechanical properties of the vagina in the active state have been exclusively studied via uniaxial tests. In these tests, either longitudinal^{4-6, 19, 27, 34} or circumferential^{16, 21, 47, 54} strips of vaginal tissue were tested, and the active forces generated by various stimulation methods were recorded. Oh *et al.*³⁵ tested both longitudinal and circumferential strips of vaginal tissue via uniaxial tests and found no significant differences in the active responses in the LD and CD³⁵. This is in contrast with the results of our biaxial tests as we found that, in response to EFS, the vagina contracted significantly more in the CD than in the LD as demonstrated by the higher active stresses in the CD (Figures 5, 6 and 9). Moreover, in response to KCl, the vagina contracted more in the LD than in the CD, generating higher active stresses in the LD (Figures 8 and 9). Before normalizing by cross sectional area, we found that our testing yielded higher, but comparable, EFS-induced active forces than tests by van Helden⁵⁴; this was expected since we used the entire vagina rather than segments. We found that the magnitudes of the active forces normalized by specimen volume generated by KCl in our tests were similar to those found in uniaxial testing¹⁹,

In our study, we measured the active mechanical response of the entire rat vagina, rather than separating it into proximal and distal regions as done by others. It has been shown that the vagina undergoes stronger contractions in the proximal than distal regions in response to EFS^{35, 47, 54} and KCl-induced stimulation^{4, 5, 35}. However, regional differences in peak active force due to KCl stimulation disappear after normalizing by cross sectional area of the smooth muscle⁴ or by weight^{35, 47}. Thus, while our biaxial tests of the entire vagina better emulated physiological loading conditions and captured the coupling effects of contractions in the LD and CD, they did not measure the heterogeneous active mechanical properties of the vagina. Future biaxial tests should be conducted by localizing the EFS or by measuring the heterogeneous deformation of the vaginal tissue using digital image correlation methods (DIC). Alternatively, square specimens for biaxial testing should be isolated from the distal and proximal regions of the vagina of large animal models.

The EFS contractions are frequency dependent, with increasing frequencies typically leading to higher active stresses^{21, 27, 35, 54}. To achieve the maximum EFS-induced contractions, we chose a frequency of 70 Hz after performing preliminary tests. The maximum EFS-induced active stresses occurred at optimal stretches, which we determined for each specimen and in both directions through our incremental stretching protocol (Figure 7). KCl-induced active stresses were measured by keeping the specimen under low equi-biaxial loads and using a high concentration of KCl (124 mM). Interestingly, there was no difference between the EFS- and KCl-induced active stresses in the CD (Figure 9). Moreover, after normalizing the maximum EFS-induced active stress by the KCl-induced active stress, the difference between the LD and CD was still found to be significant (Figure 10). This could suggest innervation mediated contractions are less dominant than receptor mediated contractions in the LD relative to the CD. It remains unknown whether these directional

differences in the active stresses are the product of the different smooth muscle content, orientation, and innervation.

There are, of course, limitations to the results found in this study. Ideally one would measure strain using non-contact measurement methods, such as digital image correlation. However, our opaque electrodes did not allow for visual inspection for strain measurement of the specimen throughout testing. Stretch was instead measured by crosshead displacement, which does not account for localized strains. In future studies, the use of transparent electrodes may allow for DIC to be utilized for more accurate strain measurements. Furthermore, our set-up did not allow for bath heating or oxygenation, which may help the specimen maintain its functionality. Finally, we chose to measure specimen thickness after testing to minimize the amount of handling prior to testing. We expect there was little change in geometry caused by the low stresses from testing. Other testing protocols in which the two directions are not stretched symmetrically may lead to more specific results, as for example in understanding the properties of the vagina during childbirth, in which one direction (circumferential) is expected to stretch more than the other (longitudinal).

In conclusion, biaxial tests are necessary to understand the complex mechanical behavior of the vaginal tissue. The effect of smooth muscle contractions has largely been ignored in previous studies on mechanical characterization of the vagina, and those who have accounted for it have done so via uniaxial tests. This study represents a springboard for future studies on the effect of pregnancy, parity, and prolapse on the passive and active biaxial mechanical behavior of vaginal tissue. The anisotropy of the vagina in its passive and active states should be considered in the development of new treatment methods for POP including vaginal meshes.

References

1. Abrams P., K. E. Andersson, L. Birder, L. Brubaker, L. Cardozo, C. Chapple, A. Cottenden, W. Davila, D. de Ridder, R. Dmochowski, M. Drake, C. DuBeau, C. Fry, P. Hanno, J. H. Smith, S. Herschorn, G. Hosker, C. Kelleher, H. Koelbl, S. Khoury, R. Madoff, I. Milsom, K. Moore, D. Newman, V. Nitti, C. Norton, I. Nygaard, C. Payne, A. Smith, D. Staskin, S. Tekgul, J. Thuroff, A. Tubaro, D. Vodusek, A. Wein and J. J. Wyndaele. Fourth international consultation on incontinence recommendations of the international scientific committee: Evaluation and treatment of urinary incontinence, pelvic organ prolapse, and fecal incontinence. *Neurourology and Urodynamics* 29: 213-240, 2010.
2. Alperin M., A. Feola, R. Duerr, P. Moalli and S. Abramowitch. Pregnancy-and delivery-induced biomechanical changes in rat vagina persist postpartum. *International Urogynecology Journal* 21: 1169-1174, 2010.
3. Badiou W., G. Granier, P.-J. Bousquet, X. Monrozies, P. Mares and R. de Tayrac. Comparative histological analysis of anterior vaginal wall in women with pelvic organ prolapse or control subjects. A pilot study. *International Urogynecology Journal* 19: 723-729, 2008.
4. Basha M., S. Chang, E. M. Smolock, R. S. Moreland, A. J. Wein and S. Chacko. Regional differences in myosin heavy chain isoform expression and maximal shortening velocity of the rat vaginal wall smooth muscle. *American Journal of Physiology-Regulatory, Integrative and Comparative Physiology* 291: R1076-R1084, 2006.
5. Basha M., E. F. LaBelle, G. M. Northington, T. Wang, A. J. Wein and S. Chacko. Functional significance of muscarinic receptor expression within the proximal and distal rat vagina. *American Journal of Physiology-Regulatory, Integrative and Comparative Physiology* 297: R1486-R1493, 2009.
6. Basha M. E., S. Chang, L. J. Burrows, J. Lassmann, A. J. Wein, R. S. Moreland and S. Chacko. Effect of estrogen on molecular and functional characteristics of the rodent vaginal muscularis. *The journal of sexual medicine* 10: 1219-1230, 2013.
7. Boreham M. K., C. Y. Wai, R. T. Miller, J. I. Schaffer and R. A. Word. Morphometric analysis of smooth muscle in the anterior vaginal wall of women with pelvic organ prolapse. *American Journal of Obstetrics & Gynecology* 187: 56-63.
8. Borges L. F., P. S. Gutierrez, H. R. C. Marana and S. R. Taboga. Picrosirius-polarization staining method as an efficient histopathological tool for collagenolysis detection in vesical prolapse lesions. *Micron* 38: 580-583, 2007.
9. Chantreau P., M. Brieu, M. Kammal, J. Farthmann, B. Gabriel and M. Cosson. Mechanical properties of pelvic soft tissue of young women and impact of aging. *International Urogynecology Journal* 25: 1547-1553, 2014.
10. Chuong C.-J., M. Ma, R. C. Eberhart and P. Zimmern. Viscoelastic properties measurement of the prolapsed anterior vaginal wall: a patient-directed methodology. *European Journal of Obstetrics and Gynecology and Reproductive Biology* 173: 106-112, 2014.
11. Dietz H. The aetiology of prolapse. *International Urogynecology Journal* 19: 1323, 2008.
12. Ellerkmann R. M., G. W. Cundiff, C. F. Melick, M. A. Nihira, K. Leffler and A. E. Bent. Correlation of symptoms with location and severity of pelvic organ prolapse. *American Journal of Obstetrics & Gynecology* 185: 1332-1338, 2001.
13. Epstein L. B., C. A. Graham and M. H. Heit. Correlation between vaginal stiffness index and pelvic floor disorder quality-of-life scales. *International Urogynecology Journal* 19: 1013-1018, 2008.

14. Epstein L. B., C. A. Graham and M. H. Heit. Systemic and vaginal biomechanical properties of women with normal vaginal support and pelvic organ prolapse. *American journal of obstetrics and gynecology* 197: 165.e161-165.e166, 2007.
15. Ettema G. J. C., J. T. W. Goh and M. R. Forwood. A new method to measure elastic properties of plastic-viscoelastic connective tissue. *Medical Engineering & Physics* 20: 308-314, 1998.
16. Feola A., S. Abramowitch, Z. Jallah, S. Stein, W. Barone, S. Palcsey and P. Moalli. Deterioration in biomechanical properties of the vagina following implantation of a high-stiffness prolapse mesh. *BJOG: An International Journal of Obstetrics & Gynaecology* 120: 224-232, 2013.
17. Feola A., S. Abramowitch, K. Jones, S. Stein and P. Moalli. Parity negatively impacts vaginal mechanical properties and collagen structure in rhesus macaques. *American journal of obstetrics and gynecology* 203: 595.e591-595.e598, 2010.
18. Feola A., R. Duerr, P. Moalli and S. Abramowitch. Changes in the rheological behavior of the vagina in women with pelvic organ prolapse. *International Urogynecology Journal* 24: 1221-1227, 2013.
19. Feola A., P. Moalli, M. Alperin, R. Duerr, R. E. Gandley and S. Abramowitch. Impact of pregnancy and vaginal delivery on the passive and active mechanics of the rat vagina. *Annals of biomedical engineering* 39: 549-558, 2011.
20. Gilchrist A. S., A. Gupta, R. C. Eberhart and P. E. Zimmern. Do Biomechanical Properties of Anterior Vaginal Wall Prolapse Tissue Predict Outcome of Surgical Repair? *The Journal of Urology* 183: 1069-1073, 2010.
21. Giraldi A., K. Persson, V. Werkström, P. Alm, G. Wagner and K. E. Andersson. Effects of diabetes on neurotransmission in rat vaginal smooth muscle. *International journal of impotence research* 13: 58, 2001.
22. Goh J. T. W. Biomechanical Properties of Prolapsed Vaginal Tissue in Pre- and Postmenopausal Women. *International Urogynecology Journal* 13: 76-79, 2002.
23. Inal H. A., P. B. Kaplan, U. Usta, E. Taştekin, A. Aybatlı and B. Tokuc. Neuromuscular morphometry of the vaginal wall in women with anterior vaginal wall prolapse. *Neurourology and Urodynamics* 29: 458-463, 2010.
24. Jallah Z. C. The role of vaginal smooth muscle in the pathogenesis of pelvic organ prolapse. University of Pittsburgh, 2014.
25. Jean-Charles C., C. Rubod, M. Brieu, M. Boukerrou, J. Fasel and M. Cosson. Biomechanical properties of prolapsed or non-prolapsed vaginal tissue: impact on genital prolapse surgery. *International Urogynecology Journal* 21: 1535-1538, 2010.
26. Jelovsek J. E. and M. D. Barber. Women seeking treatment for advanced pelvic organ prolapse have decreased body image and quality of life. *American Journal of Obstetrics & Gynecology* 194: 1455-1461.
27. Kim N., K. Min, M. Pessina, R. Munarriz, I. Goldstein and A. Traish. Effects of ovariectomy and steroid hormones on vaginal smooth muscle contractility. *International journal of impotence research* 16: 43-50, 2004.
28. Knight K. M., P. A. Moalli, A. Nolfi, S. Palcsey, W. R. Barone and S. D. Abramowitch. Impact of parity on ewe vaginal mechanical properties relative to the nonhuman primate and rodent. *International Urogynecology Journal* 27: 1255-1263, 2016.
29. Lei L., Y. Song and R. Chen. Biomechanical properties of prolapsed vaginal tissue in pre- and postmenopausal women. *International Urogynecology Journal* 18: 603-607, 2007.

30. Liang R., K. Knight, A. Nolfi, S. Abramowitch and P. A. Moalli. Differential effects of selective estrogen receptor modulators on the vagina and its supportive tissues. *Menopause* 23: 129-137, 2016.
31. Lin S.-Y., Y.-T. Tee, S.-C. Ng, H. Chang, P. Lin and G.-D. Chen. Changes in the extracellular matrix in the anterior vagina of women with or without prolapse. *International Urogynecology Journal* 18: 43-48, 2007.
32. Lopez S. O., R. C. Eberhart, P. E. Zimmern and C.-J. Chuong. Influence of body mass index on the biomechanical properties of the human prolapsed anterior vaginal wall. *International Urogynecology Journal* 26: 519-525, 2015.
33. Moalli P. A., S. H. Shand, H. M. Zyczynski, S. C. Gordy and L. A. Meyn. Remodeling of vaginal connective tissue in patients with prolapse. *Obstetrics & Gynecology* 106: 953-963, 2005.
34. Northington G. M., M. Basha, L. A. Arya, A. J. Wein and S. Chacko. Contractile response of human anterior vaginal muscularis in women with and without pelvic organ prolapse. *Reproductive Sciences* 18: 296-303, 2011.
35. Oh S., S. Hong, S. Kim and J. Paick. Histological and functional aspects of different regions of the rabbit vagina. *International journal of impotence research* 15: 142-150, 2003.
36. Olsen A. L., V. J. Smith, J. O. Bergstrom, J. C. Colling and A. L. Clark. Epidemiology of surgically managed pelvic organ prolapse and urinary incontinence. *Obstetrics & Gynecology* 89: 501-506, 1997.
37. Patnaik S. S., B. Brazile, V. Dandolu, M. Damaser, C. van der Vaart and J. Liao. Sheep as an animal model for pelvic organ prolapse and urogynecological research. In: *ASB 2015 Annual Conference*.
38. Peña E., B. Calvo, M. A. Martínez, P. Martins, T. Mascarenhas, R. M. N. Jorge, A. Ferreira and M. Doblaré. Experimental study and constitutive modeling of the viscoelastic mechanical properties of the human prolapsed vaginal tissue. *Biomechanics and Modeling in Mechanobiology* 9: 35-44, 2010.
39. Peña E., P. Martins, T. Mascarenhas, R. M. Natal Jorge, A. Ferreira, M. Doblaré and B. Calvo. Mechanical characterization of the softening behavior of human vaginal tissue. *Journal of the Mechanical Behavior of Biomedical Materials* 4: 275-283, 2011.
40. Rahn D. D., M. D. Ruff, S. A. Brown, H. F. Tibbals and R. A. Word. Biomechanical Properties of The Vaginal Wall: Effect of Pregnancy, Elastic Fiber Deficiency, and Pelvic Organ Prolapse. *American journal of obstetrics and gynecology* 198: 590.e591-590.e596, 2008.
41. Robison K. M., C. K. Conway, L. Desrosiers, L. R. Knoepp and K. S. Miller. Biaxial Mechanical Assessment of the Murine Vaginal Wall Using Extension-Inflation Testing. *Journal of Biomechanical Engineering* 139: 104504-104504-104508, 2017.
42. Röhrnbauer B., C. Betschart, D. Perucchini, M. Bajka, D. Fink, C. Maake, E. Mazza and D. A. Scheiner. Measuring tissue displacement of the anterior vaginal wall using the novel aspiration technique in vivo. *Scientific reports* 7: 16141, 2017.
43. Rubod C., M. Boukerrou, M. Brieu, P. Dubois and M. Cosson. Biomechanical Properties of Vaginal Tissue. Part 1: New Experimental Protocol. *The Journal of Urology* 178: 320-325, 2007.
44. Rubod C., M. Boukerrou, M. Brieu, C. Jean-Charles, P. Dubois and M. Cosson. Biomechanical properties of vaginal tissue: preliminary results. *International Urogynecology Journal* 19: 811-816, 2008.

45. Rubod C., M. Brieu, M. Cosson, G. Rivaux, J.-C. Clay, L. de Landsheere and B. Gabriel. Biomechanical Properties of Human Pelvic Organs. *Urology* 79: 968.e917-968.e922, 2012.
46. Rynkevicius R., P. Martins, L. Hympanova, H. Almeida, A. A. Fernandes and J. Deprest. Biomechanical and morphological properties of the multiparous ovine vagina and effect of subsequent pregnancy. *Journal of biomechanics* 57: 94-102, 2017.
47. Skoczylas L. C., Z. Jallah, Y. Sugino, S. E. Stein, A. Feola, N. Yoshimura and P. Moalli. Regional differences in rat vaginal smooth muscle contractility and morphology. *Reproductive Sciences* 20: 382-390, 2013.
48. Subak L. L., L. E. Waetjen, S. Van Den Eeden, D. H. Thom, E. Vittinghoff and J. S. Brown. Cost of pelvic organ prolapse surgery in the United States. *Obstetrics & Gynecology* 98: 646-651, 2001.
49. Takacs P., M. Gualtieri, M. Nassiri, K. Candiotti and C. A. Medina. Vaginal smooth muscle cell apoptosis is increased in women with pelvic organ prolapse. *International Urogynecology Journal* 19: 1559, 2008.
50. Tokar S., A. Feola, P. A. Moalli and S. Abramowitch. Characterizing the biaxial mechanical properties of vaginal maternal adaptations during pregnancy. In: *ASME 2010 Summer Bioengineering Conference* American Society of Mechanical Engineers, 2010, p. 689-690.
51. Ulrich D., S. L. Edwards, V. Letouzey, K. Su, J. F. White, A. Rosamilia, C. E. Gargett and J. A. Werkmeister. Regional variation in tissue composition and biomechanical properties of postmenopausal ovine and human vagina. *PloS one* 9: e104972, 2014.
52. Ulrich D., S. L. Edwards, K. Su, J. F. White, J. A. M. Ramshaw, G. Jenkin, J. Deprest, A. Rosamilia, J. A. Werkmeister and C. E. Gargett. Influence of Reproductive Status on Tissue Composition and Biomechanical Properties of Ovine Vagina. *PloS one* 9: e93172, 2014.
53. Urbankova I., G. Callewaert, S. Blacher, D. Deprest, L. Hympanova, A. Feola, L. De Landsheere and J. Deprest. First delivery and ovariectomy affect biomechanical and structural properties of the vagina in the ovine model. *International Urogynecology Journal* 1-10, 2018.
54. van Helden D. F., A. Kamiya, S. Kelsey, D. R. Laver, P. Jobling, R. Mitsui and H. Hashitani. Nerve-induced responses of mouse vaginal smooth muscle. *Pflügers Archiv-European Journal of Physiology* 1-13, 2017.
55. Wijeratne R. S., R. D. Vita, J. A. Rittenhouse, E. B. Orler, R. B. Moore and D. A. Dillard. Biaxial properties of individual bonds in thermomechanically bonded nonwoven fabrics. *Textile Research Journal* 0040517517753640, 2018.